MOBILE DOPPLER RADAR OBSERVATIONS OF TORNADOES

Howard B. Bluestein

School of Meteorology, University of Oklahoma, 120 David L. Boren Blvd., Suite 5900, Norman, Oklahoma 73072, U. S. A., hblue@ou.edu

...

(Dated: April 16, 2007)

I. INTRODUCTION

Over the past decade, our research group has been using truck-mounted Doppler radars from the University of Massachusetts to learn how tornadoes form and to map the wind field in them and in dust devils (see reference list). Remote sensing of the reflectivity and wind fields associated with tornadoes has proven to be a safe and effective way of documenting tornado behavior and structure. It is necessary to get relatively close to tornadoes, because at long range the near-surface portion of the tornado lies underneath the radar beam and the spatial resolution is degraded owing to beam spreading, and it is useful to be close enough to obtain simultaneous visual imagery.

The purpose of this presentation is to highlight the most significant results from our recent field programs (since 1999). Results not related to intense atmospheric vortices and results from field programs using other mobile Doppler radars (e.g., IHOP, the DOWs, the SMART-Rs, etc.) are detailed elsewhere.

II. PRESENTATION OF RESEARCH

The analyses summarized herein are based on data collected by a W-band (3-mm wavelength) radar and a polarimetric, X-band (3-cm wavelength) radar. The former has a half-power beamwidth of only 0.18º, which allows for an azimuthal resolution ~ 10 m at 3 km range. The pulse length is either 15 m or 30 m, depending on the sensitivity required; W-band radiation is severely attenuated in the presence of precipitation. The latter has a half-power beamwidth of 1.25º, which allows for a coarser look at a broader area surrounding the tornado. Polarization diversity allows for an analysis of the type of scatterer in the radar volume; in a tornado, it is possible to discriminate between raindrops and debris (Ryzhkov et al. 2005).

III. RESULTS AND CONCLUSIONS

The most important findings from our recent field programs are as follows:

a. Tornadogenesis in one case was found to follow a 0.5 km - scale jet-like burst along the rear-flank gust front, which produced a small-scale bow-echo-like feature; coincidentally, a vortex formed along its leading edge. The vortex then interacted with a larger-scale vortex and evolved into a tornado.

b. The reflectivity distribution inside tornadoes near the ground had a 100-m scale weak-echo hole, which closed up in the lowest few tens of meters above the ground. The wind speed in the core of one tornado decreased from a maximum ~ 25 m AGL (~ 78 m s^{-1}) by ~ 20 – 25% from that at the ground. Horizontal vortices were evident along one side of the tornado vortex and a jet of outflow was found ~ 100 m AGL on the other side. Radial bulges in the weak-echo eye were found in a few tornadoes.

c. The inner ring of reflectivity in tornadoes appears to be caused by scattering from airborne debris particles, while outer spiral bands are caused by precipitation particles.

d. The radial distribution of wind in tornadoes is like that in a Burgers – Rott vortex. Questions still remain about the representativeness of scatterer motion as tracers of the wind field when centrifuging is significant.

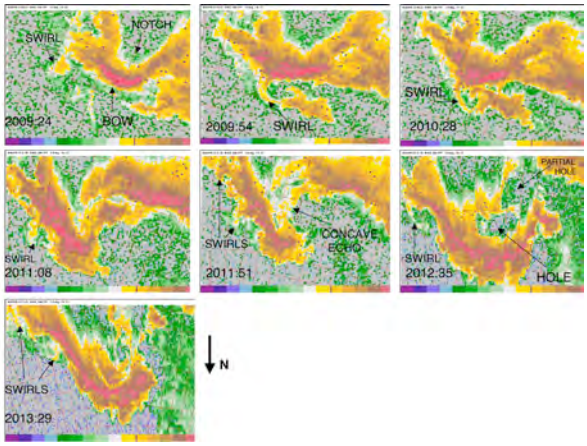

FIG. 1: Depiction of the evolution of radar reflectivity in a developing tornado. Data from the U. Mass. W-band radar. From Bluestein et al. (2003a)

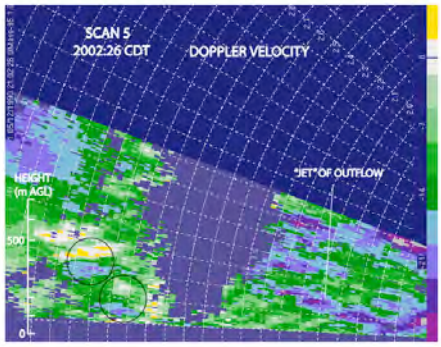

FIG. 2: Vertical cross section of Doppler velocity (m s^{-1}) through the center of a tornado during its mature stage. Data from the U. Mass. W-band radar. From Bluestein et al. (2007a).

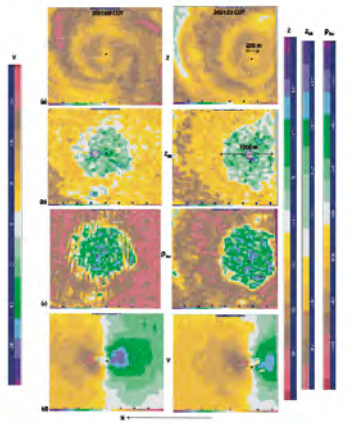

FIG. 3: Horizontal cross sections of (a) radar reflectivity factor (dBZ), (b) differential reflectivity Z_{DR} (dB), (c) cross-correlation coefficient (ρ_{HV}), and (d) Doppler velocity (m s^{-1}) in a mature tornado. Data from the U. Mass. X-band radar. From Bluestein et al. (2007b).

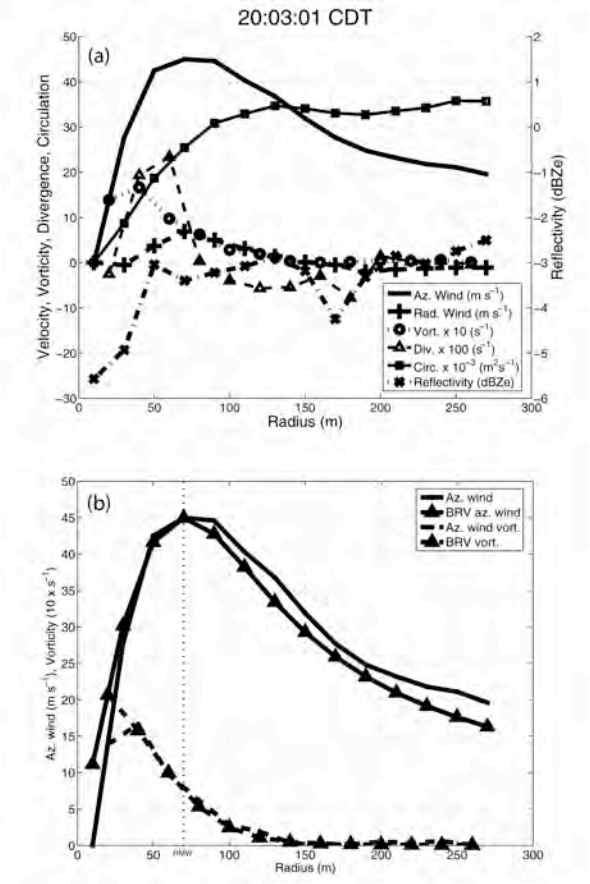

FIG. 4: (a) Radial profile of GBVTD- (ground-based velocity track display) analyzed azimuthally averaged azimuthal velocity (m s^{-1}), radial velocity (m s^{-1}), vorticity X 10 (s^{-1}), divergence X 100 (s^{-1}), circulation X 10^{-3} ($m^2 s^{-1}$), and reflectivity (dBZ_e) for a tornado during its mature stage. Positive radial velocity indicates flow away from the tornado vortex center. (b) Radial profile of GBVTD-analyzed azimuthally averaged azimuthal velocity (solid curve), the azimuthal velocity profile of a Burgers – Rott vortex (BRV) with the same maximum velocity and RMW (radius of maximum wind) (solid curve with triangle markings). The vorticity assoicted with each of the profiles (multiplied by a factor of 10 for clarity) is indicated by broken lines with corresponding symbols. Based on data from the U. Mass. W-band radar. (from Tanamachi et al. 2007)

IV. AKNOWLEDGMENTS

Personnel at the Microwave Remote Sensing Laboratory (MRSL) at the University of Massachusetts provided the mobile radars and support. Graduate students at the University of Oklahoma and University of Massachusetts participated in our field programs and processed the data. Andy Pazmany (ProSensing, Inc.) and Steve Frasier (MRSL) are acknowledged for their important roles in providing us with use of the radars. The research summarized in this abstract was supported by NSF Grants ATM-9616730, ATM-0241037, and ATM-0637148.

V. REFERENCES

Bluestein, H. , 2005: A review of ground-based, mobile, W-band, Doppler-radar observations of tornadoes and dust devils. *Dyn. of Atmospheres and Oceans*, **40**, 163 – 188.

Bluestein, H. B., and A. L. Pazmany, 2000: Observations of tornadoes and other convective phenomena with a mobile, 3-mm wavelength, Doppler radar: The spring 1999 field experiment. *Bull. Amer. Meteor. Soc.*, **81**, 2939 – 2951.

Bluestein, H. B., C. C. Weiss, and A. L. Pazmany, 2003: Mobile-Doppler-radar observations of a tornado in a supercell near Bassett, Nebraska on 5 June 1999. Part I: Tornadogenesis. *Mon. Wea. Rev.*, **131**, 2954 – 2967.

Bluestein, H. B., C. C. Weiss, A. L. Pazmany, W.-C. Lee, and M. Bell, 2003: Mobile-Doppler-radar observations of a tornado in a supercell near Bassett, Nebraska on 5 June 1999. Part II: Tornado-vortex structure. *Mon. Wea. Rev.*, **131**, 2968 – 2984.

Bluestein, H. B., C. C. Weiss, and A. L. Pazmany, 2004: Dopper-radar observations of dust devils in Texas. *Mon. Wea. Rev.*, **132**, 209 – 224.

Bluestein, H. B., C. C. Weiss, and A. L. Pazmany, 2004: The vertical structure of a tornado near Happy, Texas on 5 May 2002: High-resolution, mobile, W-band, Doppler-radar observations. *Mon. Wea. Rev.*, **132**, 2325 – 2337.

Bluestein, H. B., C. C. Weiss, M. M. French, E. Holthaus, R. L. Tanamachi, S. Frasier, and A. L. Pazmany, 2007: The structure of tornadoes near Attica, Kansas on 12 May 2004: High-resolution, mobile, Doppler-radar observations. *Mon. Wea. Rev.*, **135**, 475 – 506.

Bluestein, H. B., M. M. French, R. L. Tanamachi, S. Frasier, K.Hardwick, F. Junyent, and A. L. Pazmany, 2007: Close-range observations of tornadoes in supercells made with a dual-polarization, X-band, mobile Doppler radar. *Mon. Wea. Rev.*, **135**, 1522 – 1543.

Ryzhkov, A. V., T. J. Schuur, D. W. Burgess, and D. S. Zrnic, 2005: Polarimetric tornado detection. *J. Appl. Meteor.*, **44**, 557 – 570.

Tanamachi, R. L., H. B. Bluestein, W.-C. Lee, M. Bell, and A. Pazmany, 2007: Ground-based velocity display (GBVTD) analysis of W-band Doppler radar data in a tornado near Stockton, Kansas on 15 May 1999. *Mon. Wea. Rev.*, **135**, 783 – 800.